Internal Coordinate Modeling of DNA: Force Field Comparisons

DELPHINE FLATTERS, KRYSTYNA ZAKRZEWSKA, RICHARD LAVERY

Lavoratoire de Biochimie Théorique, CNRS URA 77, Institut de Biologie Physico-Chimique 13, rue Pierre et Marie Curie, Paris 75005, France

Received 12 August 1996; accepted 16 October 1996

ABSTRACT: The Jumna internal coordinate program for modeling nucleic acids was extended to include the force field developed for the Amber program. This forms a bridge between internal and Cartesian coordinate modeling approaches. Using the extensive conformational mapping and substate search facilities available within Jumna, we rigorously compared the behavior of the different force fields and also of different continuum solvent models. The results, which help to explain trends seen in earlier minimization and molecular dynamics simulations, point to the superiority of the latest Amber parameterization (Parm94) and to a surprising degree of agreement with the Flex force field originally developed for Jumna. © 1997 by John Wiley & Sons, Inc. *J Comput Chem* **18**: 1043–1055, 1997

Keywords: molecular; modeling; nucleic acids; solvent models; parameterization

Introduction

The structure and the ionic nature of nucleic acids makes them notoriously sensitive to their environment. This experimental fact is reflected by difficulties in modeling nucleic acid oligomers, which, during molecular dynamic simulations, can easily undergo severe deformation or even partial denaturation. Although results obtained with explicit water generally behave better (notably, when the truncation of long-range electrostatic interactions is avoided[1, 2] these calculations are very costly. Consequently, they cannot be easily be used for many biologically important problems such as large-scale structural deformations, systematic studies of base sequence effects, or ligand/protein docking. It thus remains important to optimize simulation techniques that avoid dealing with explicit water.

One of the difficulties in searching for the best simulation conditions is that, in the case of macromolecules, energy minimization in Cartesian coordinates is generally inefficient, rapidly becoming trapped in local minima and seldom leading to more than a relaxation of steric hindrance (see, for example, refs. 3, 4). It is thus difficult to make a thorough investigation of the energy hypersurface produced by a given set of force field parameters.

Correspondence to: R. Lavery

CCC 0192-8651 / 97 / 081043-13

One way of overcoming this problem is to change coordinates and to work with internal variables (bond lengths, bond angles, and dihedrals). This change to a chemically meaningful coordinate set enables stiffer degrees of freedom to be separated and frozen, strongly reducing the dimensionality of the space to be studied and concurrently reducing the number of local minima.

In the case of the nucleic acids, such an approach was implemented in JUMNA (junction minimization of nucleic acids),[5,6] which enabled both sequence-dependent fine structure[7,8] and major conformational changes[5,9,10] to be studied. We can also use this program as a test bed for comparing force fields and simplified solvent representations. The present article presents results concerning the original force field developed for JUMNA, termed Flex,[5,11,12] and the two force fields developed for AMBER (assisted model building with energy refinement).[13,14] The choice of AMBER for this comparison was guided by two facts: AMBER is the most widely used code for molecular dynamics simulations of nucleic acids and its authors recently presented a new and refined force field (specifically conceived for simulations in explicit water).

As well as forming a bridge between internal coordinate and Cartesian coordinate modeling approaches, the extension of JUMNA allows us to use its specialized tools for comparing the chosen force fields. The most important of these possibilities are constrained adiabatic conformational mapping and a combinatorial technique for rapidly locating stable conformational substates. Combined with the possibility of treating helically symmetric nucleic acid polymers, these approaches allow us to make a thorough study of the conformational space of helical DNAs for different base sequences and for different allomorphic forms.

We also study the impact of various continuum models of solvent and counterions on each force field. Solvent electrostatic damping is represented using distance-dependent dielectric functions, which vary either linearly or sigmoidally with distance. Counterion damping is modeled by reducing the net charge of each anionic phosphate group. Explicit counterions are not considered because experience shows that freely moving counterions are not compatible with efficient energy minimization, while counterions rigidly fixed to phosphate groups can radically modify the conformation behavior of DNA (notably, for states with narrow grooves such as A-DNA[7,15]).

Methodology

JUMNA[5,6] models DNA by breaking each strand down into a series of 3′-monophosphate nucleotides (with the exception of the 3′ terminal nucleotide that does not carry a phosphate group and ends C3′—OH). The internal flexibility of each nucleotide is described by nine variables: the glycosidic rotation, 4-variable sugar puckering, two backbone dihedrals ε(C4′—C3′—O3′—P) and ζ (C3′—O3′—P—O5), and two valence angles (C3′—O3′—P) and (O3′—P—O5′). The nucleotides are positioned in space with respect to a common helical axis system using three translational variables (Xdisp, Ydisp, and rise) and three rotational variables (inclination, tip, and twist). The chemical bonds between successive nucleotides (O5′—C5′) are maintained by strong harmonic constraints. This model corresponds to freezing all bond lengths and maintaining rigid bases, while all single bond rotations are allowed and valence angles are variable within the sugar rings and along the phosphodiester backbone.

For nucleic acid oligomers, JUMNA requires roughly 10 times fewer variables than standard Cartesian coordinate models. Although this is already a considerable reduction, it is possible to go further still for DNAs with regular repeating base sequences. In such cases, we can impose helical symmetry and optimize the energy of a single repeating unit, rather that the energy of the whole molecule. If we consider alternating poly(dG-dC) · poly(dG-dC) as an example, the repeating unit is a double stranded GpCp dinucleotide. Obtaining the structure of such a polymer requires optimizing the structure of this subunit as a function of its energy within a polymeric environment E:

$$E = E_{00} + 1/2 \sum_{\substack{i=-\infty,\\ i\neq 0}}^{\infty} E_{0i} = \sum_{i=0}^{\infty} E_{0i}$$

(because by helical symmetry $E_{0-i} = E_{0i}$) where E_{00} is the internal energy of the repeating unit and E_{0i} is its interaction energy with the ith unit of the polymer.

In fact, it is possible to truncate this sum once the optimal structure is stable with respect to the addition of further nucleotides. In the present work, dinucleotide repeating sequences are treated using 17 nucleotide pairs interacting with the basic dinucleotide repeating unit.

Using this approach, we not only greatly reduce the time necessary for energy calculations, but we also reduce the number of variables again to only 30 for the example given (remembering that this polymer has a dyadic symmetry within each of its repeating units). This very significant simplification (roughly 20 times fewer variables than for a single turn of DNA treated in Cartesian space) effectively makes it feasible to fully investigate the conformational space of the polymer and, notably, to locate all the stable conformational states close to the canonical forms of the double helix.

To automate conformational searches with JUMNA, we developed two related techniques. The first consists of adiabatic mapping in 1 or 2 dimensions with respect to any chosen internal or helicoidal variables. The maps we use here concern sugar puckering and, more specifically, sugar phase angle. Earlier studies with JUMNA showed that sugar puckering is very important in fixing the overall conformation of the double helix,[7,8] and indeed every conformational substate that we located can be uniquely labeled by simply describing its sugar puckers. (These puckers can in grouped into four families termed: S, low amplitude C2′-*endo*, X, high amplitude C2′-*endo*; E; O4′-*endo*; and N, C3′-*endo*.) Consequently mapping out the energy surface of DNA as a function of it sugar puckers gives insight into its conformational substates and into the transition pathway between its common A and B allomorphs.[8]

Within JUMNA sugar phase angles (P) can be constrained, independently from the amplitude of puckering (A), by deriving the pseudorotational equations proposed by Rao et al.[16] and converting the resulting derivatives into an ensemble of torques acting on the endo-cyclic dihedral angles of the sugars.

Mapping is naturally limited to problems involving only one or two significant variables [e.g., the two independent sugar phases within helically symmetric poly(dG-dC) · poly(dG-dC)]. When there are more variables to treat another technique can be employed. Recalling that all the stable conformations we detect can be characterized by their sugar puckering, we developed an automated combinatorial search that generates B-DNA starting structures with all possible combinations of sugar puckers (S, X, and, for pyrimidines, E). These starting structures are then energy minimized and the results are clustered to determine how many unique conformations were located.[8,17] This approach is used in the present work to locate the substates of a polymeric DNA with a tetranucleotide repeating sequence, $(AGAT)_n$. This polymer contains eight symmetry distinct sugars.

We also calculated the macroscopic twisting and bending moduli of DNA and compared these data with available experimental results as a function of base sequence, force field, and solvent model.

The force fields that we compare are Flex,[6] the standard force field used in JUMNA, and two AMBER force fields, the original parameterization due to Weiner et al.[13] and the recent version proposed by Cornell et al.[14] For brevity, these two force fields are referred to as Parm91 and Parm94, following the notation used within the AMBER program.

Using a coherent notation these two force fields can be written as follows:

$$E_{\text{flex}} = \sum_{nb}\left(\frac{q_i q_j}{\varepsilon r_{ij}} + \frac{A_{ij}}{r_{ij}^{12}} - \frac{B_{ij}}{r_{ij}^{6}}\right) + \sum_{\phi}\frac{V_\phi}{2} \times[1 + \cos(n\phi - \gamma)] + \sum_{\theta} k_\theta(\theta - \theta_{\text{eq}})^2 + \sum_{l} K_l(l - l_{\text{eq}})^2 + \sum_{HB}\cos\,\theta_{HB}\left[\left(\frac{A_{ij}^{\text{HB}} - A_{ij}}{r_{ij}^{12}}\right) - \left(\frac{B_{ij}^{\text{HB}} - B_{ij}}{r_{ij}^{6}}\right)\right],$$

$$E_{\text{Amber}} = \sum_{nb} f_{ij}^{\text{el}}\left(\frac{q_i q_j}{\varepsilon r_{ij}}\right) + f_{ij}^{vdw}\left(\frac{A_{ij}}{r_{ij}^{12}} - \frac{B_{ij}}{r_{ij}^{6}}\right) + \sum_{\varnothing}\frac{V_\gamma}{2}[1 + \cos(n\phi - \gamma)] + \sum_{\theta} k_\theta(\theta - \theta_{\text{eq}})^2 + \sum_{l} K_l(l - l_{\text{eq}})^2 + \sum_{\text{HB}}\left(\frac{A_{ij}^{\text{HB}}}{r_{ij}^{12}} - \frac{B_{ij}^{\text{HB}}}{r_{ij}^{10}}\right).$$

These two formulations differ only slightly. The first four terms of each equation describe, respectively, nonbonded electrostatic (el) and van der Waals (vdW) interactions (between all unique atom pairs i, j separated by at least three chemical bonds), dihedral bond rotations (ϕ), valence angle deformations (θ), and bond length (l) deformations. In the case of the Flex force field, the last term adds an angular dependence to hydrogen bonding interactions that decreases their strength as the angle A-H $\cdots$ B (θ_{HB}) deviates from 180°. In the case of AMBER, the nonbonded parameters carry special weighting terms when the interac-

tions involve atoms separated by exactly three chemical bonds (in Parm91, $f^{el} = f^{vdW} = 1/2$, while in Parm94, $f^{el} = 1/1.2$ and $f^{vdW} = 1/2$). With the earlier parameterization of AMBER there is also a special hydrogen bonding term employing a 12–10 distance dependence.

Despite the similarity of the formulae, the majority of the parameters differ considerably between the Flex and AMBER force fields, and there are also nonnegligible changes between Parm91 and Parm94. This is particularly true of the atomic charges that generally decrease in polarity in the order Parm91 > Parm94 > Flex. An example of this trend is shown in Table I for the case of a cytidine nucleotide. However, such differences are not unexpected. The simplified nature of molecular mechanics force fields always leads to compensations between different terms, implying that very different parameter sets may finally lead to similar results.

To model environmental effects, we use two common strategies. First, counterion interactions are modeled by reducing the net charge on each phosphate group (by adding a chosen point charge to each of the anionic oxygens). Three cases are considered: a full net charge of -1.0, a half charge -0.5, and a quarter charge -0.25, corresponding to the value obtained by Manning's counterion condensation theory under physiological conditions.[18] Second, solvent electrostatic damping is modeled using a distance-dependent dielectric function. The simplest form of this function is $\varepsilon = r$, where r is the distance in (Ångstroms) separating two interacting point charges. Damping can be increased by adding a factor, as in the function $\varepsilon = 4r$. Both of these formulations have commonly been used with AMBER simulations. Alternatively, it was suggested, on the basis of simple electrostatic models,[19] that a sigmoidal function could be more appropriate. One such formulation is given below,[5]

$$\varepsilon(r) = \frac{(D-1)}{D}[(rs)^2 + 2rs + 2]\exp(-rs),$$

where D is the plateau value of the dielectric reached at long distances and s is the slope of the sigmoidal function. This function fits the original form proposed by Hingerty et al.[19] if $s = 0.356$, but a smaller value of 0.16 was also commonly employed within JUMNA[5,7–10] and found to yield B-DNA structures in good agreement with experimental results. The sigmoidal form of the dielectric function was also programmed[20] and successfully used within Amber.[21] Figure 1 compares these different formulations and also shows that there is a certain similarity between $\varepsilon = r$ and the sigmoidal function with $s = 0.16$, and between $\varepsilon = 4r$ and the sigmoidal function with $s = 0.356$. However, the sigmoidal function always leads to less damping at short distances, notably around 2–3Å, where hydrogen bonding interactions occur. The impact of these different choices is discussed in the Results.

For the purposes of comparing force fields and solvent/counterion models, we chose two regular repeating sequences, poly(dA-dT) · poly(dA-dT) and poly(dG-dC) · poly(dG-dC). NMR data shows that alternating Pur-Pyr tracts adopt conformations in solution belonging to the B-DNA family. However, both sequences are also able to undergo a B–A transition.

TABLE I.
Atomic Charges for a 3′-Monophosphate Nucleotide, Cytidine, Within Different Force Fields Studied.

Atom	Parm91	Parm94	Flex
C1′	0.3760	−0.0116	0.2946
C2′	−0.3070	−0.0854	−0.0665
C3′	0.2330	0.0173	0.0463
C4′	0.0360	0.1629	0.1258
O1′	−0.3680	−0.3691	−0.3341
C5′	0.1180	−0.0069	−0.0136
H1′	0.0090	0.1963	0.0641
H2′	0.0810	0.0718	0.0523
H2″	0.0810	0.0718	0.0523
H3′	0.0250	0.0985	0.0634
H4′	0.0560	0.1176	0.0605
H5′	0.0210	0.0754	0.0666
H5″	0.0210	0.0754	0.0666
O3′	−0.5090	−0.5232	−0.2806
P	1.3850	1.1659	0.4561
O5′	−0.5090	−0.4954	−0.2780
O1P	−0.8470	−0.7761	−0.5801
O2P	−0.8470	−0.7761	−0.5801
N1	−0.1870	−0.0339	−0.2403
C6	0.1850	−0.0183	0.2516
O2	−0.5080	−0.6548	−0.4474
N3	−0.8600	−0.7748	−0.5182
C4	0.9350	0.8439	0.4066
N4	−0.8340	−0.9773	−0.5605
C5	−0.5760	−0.5222	−0.2791
C2	0.8590	0.7959	0.4687
H1N4	0.3290	0.4314	0.2946
H2N4	0.3510	0.4314	0.2946
HC5	0.1530	0.1863	0.0549
HC6	0.0980	0.2293	0.0596

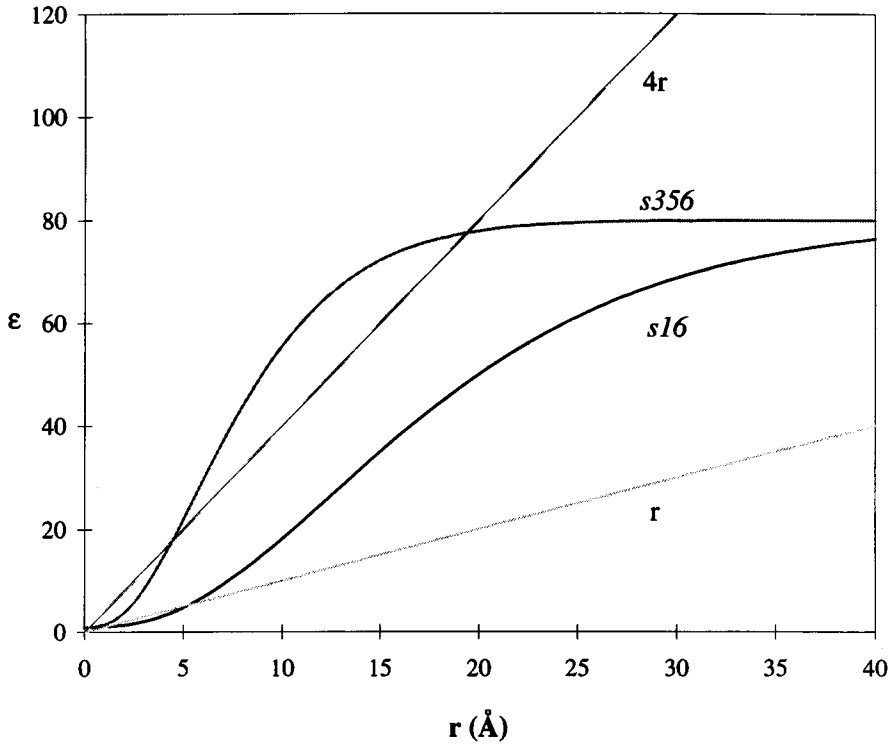

FIGURE 1. Comparison of different distance-dependent dielectric functions.

Results

CONFORMATIONAL MAPPING

The presence of stable conformational states in the space spanning the A and B forms of DNA was studied using adiabatic mapping. The variables for these maps were the two unique sugar phase angles of the test polymers, poly(dG-dC) · poly(dG-dC) and poly(dA-dT) · poly(dA-dT) (abbreviated as GC and AT, respectively). Each map covers phase angles for the purine and pyrimidine nucloeotides between 0° and 190° with energy optmizations being performed at intervals of 10°. Each map therefore contains 400 data points and requires roughly 24 h of computation on an HP 9000/735 workstation. Maps were calculated for both polymers using the three force fields under study (Parm91, Parm94, and Flex), three different phosphate net charge (-0.1, -0.5, -0.25), and four dielectric functions (r, $4r$, sigmoidal $s = 0.16$, abbreviated as *s16*, and sigmoidal $s = 0.356$, abbreviated as *s356*). Several examples of these maps are given in Figure 2 for the case of the GC polymer. The energies and conformational characteristics of the principle minima on each map are summarized in Tables II–IV. For each map, the minima are listed in order of increasing sugar phase angles (corresponding to the A → B direction along the trailing diagonal of the maps in Fig. 2). Hybrid conformations[17] containing mixed sugar puckers are only listed if they are more stable than either the A or B forms.

This data enables us to eliminate a number of simulation conditions rather easily. In order for a given force field and solvent model to be judged acceptable, we first expect to see stable conformations in the B-DNA region of the map (C2′-*endo* sugars, top right-hand corner, Fig. 2) with helical parameters within the range typically covered by the B-family.[22] We would also expect to see a local minimum in the A-DNA region with A-like conformational parameters (C3′-*endo* sugars, bottom left corner of the map, Fig. 2), although it should be less stable than the B-form for these sequences. It should be recalled that the A conformation can be easily induced by an admixture of less polar solvent or by protein interactions[23–25] and that it can also coexist with B-DNA within a crystal environment.[26] Ideally, we would therefore like to detect both A and B forms and to be able to regulate their relative stabilities. Note lastly that crystallo-

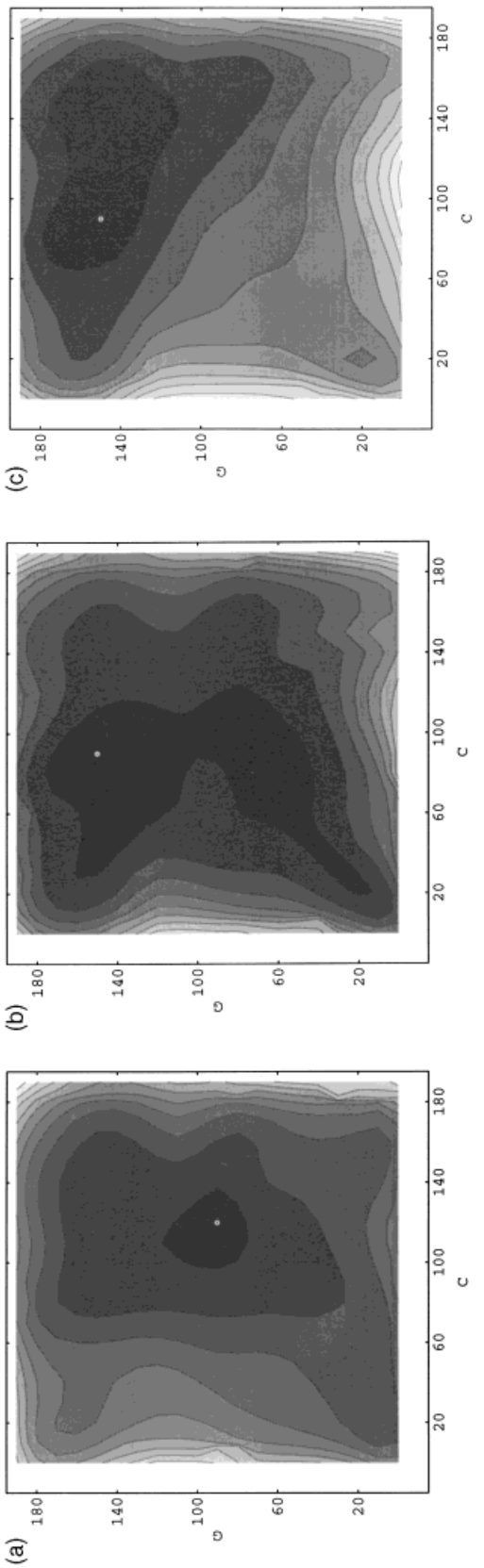

Figure 2. Energy sufaces as a function of sugar phase angles (C; cytidine; G; guanidine) within poly(dG-dC) · poly(dG-dC). Darker shading corresponds to more negative energies. The total energy range in each graphic is roughly 20 kcal/mol). (a) Parm91, $\varepsilon = r$, phos = −1.0; (b) Parm91, $\varepsilon = 4r$, phos = −1.0; (c) Parm94, $\varepsilon = 4r$, phos = −1.0; (d) Flex, $\varepsilon = 4r$, phos = −1.0; and (e) Parm94, $\varepsilon = s356$, phos = −0.5; (f) Flex, $\varepsilon = s356$, phos = −0.5.

TABLE II.
Stable Helical Conformations with AMBER-91.

		GC							AT						
Diel.	Phase	Xdisp	Inc	Prop	Rise	Twist	ΔE	Phase	Xdisp	Inc	Prop	Rise	Twist	ΔE
Phosphate charge −1.0														
r	10, 30	−0.8	−30	7.0	4.3 / 5.3	30 / 29	2.5	10, 20	−1.4	−27	4	4.2 / 5.1	30 / 29	0.1
	90, 120	−3.3	−17	15.0	4.1 / 4.2	29 / 28	0	140, 90	−3.5	−9	7	4.0 / 3.5	28 / 32	0
	140, 120	−3.1	−16	15.3	4.4 / 3.8	31 / 30	0.4							
4r	30, 30	−5.2	−5	1	3.3 / 4.2	27 / 25	1.2	20, 20	−4.6	−10	5	3.5 / 4.6	29 / 24	0.7
	150, 90	−3.3	3	−13	3.2 / 2.8	34 / 33	0	150, 90	−3.1	2	−15	3.3 / 2.7	33 / 33	0
s16	10, 20	−1.1	−26	−1	3.9 / 5.1	33 / 28	12.4							
								80, 160	−2.5	7.4	−12	2.7 / 3.6	36 / 30	0
								140, 160	−2.3	8.7	−8.8	2.8 / 3.5	41 / 28	0.4
	180, 150	−1.6	6	−3	2.8 / 3.4	31 / 45	0	180, 150	−1.8	4.1	1.8	2.9 / 3.5	29 / 45	0.6
s356	20, 20	−4.8	−6	−2	3.3 / 4.0	29 / 26	1.8	10, 10	4.4	−8	−1	3.5 / 3.9	28 / 29	0.7
	150, 90	−3.6	2	−8	3.3 / 2.9	31 / 33	0	140, 90	−4.2	3	−5	3.1 / 3.0	29 / 33	0
Phosphate charge −0.5														
r	20, 20	−4.6	−8.0	−1	3.4 / 4.1	29 / 26	1.7	10, 10	−4.4	−7	−2	3.5 / 3.8	28 / 29	0.1
	150, 90	−3.5	1.0	−5	3.4 / 2.9	30 / 34	0	140, 90	4.2	2	−3	3.3 / 3.0	28 / 32	0
	180, 150	−1.7	5.8	−7	2.9 / 3.2	32 / 44	2.8							
4r	20, 20	−5.1	12	−18	2.4 / 3.1	29 / 32	0.6	20, 20	−4.8	17	−22	2.2 / 3.0	31 / 33	0.1
	150, 40	−3.8	14	−19	2.9 / 2.4	44 / 23	0	140, 50	4.3	16	−20	2.7 / 2.5	40 / 24	0
	150, 90	−3.5	8	−14	3.0 / 2.7	35 / 32	0	140, 90	−3.8	9	−16	2.9 / 2.6	34 / 31	0.5
s16	10, 10	−4.7	1.0	−8.0	3.0 / 3.5	30 / 31	6.8	10, 10	−4.7	9.4	−14	2.8 / 3.0	31 / 33	0.4
								70, 20	−3.5	15	−22	2.7 / 3.3	40 / 25	0
	150, 150	−2.1	3.9	−5.1	3.3 / 2.8	41 / 32	3.1							
	180, 150	−1.7	9.0	−5.0	2.6 / 3.3	31 / 45	0	180, 140	−2.1	8	−3	2.7 / 3.3	28 / 45	3.0
s356	20, 20	−5.1	14	−18	2.4 / 3.0	32 / 31	0	20, 20	−4.8	21	−22	2.1 / 2.8	33 / 33	
	170, 150	2.3	7.7	−9.5	2.8 / 3.0	35 / 40	2.7							
	150, 160	−2.6	4.9	−8	3.0 / 2.9	40 / 32	2.5							
Phosphate charge −0.25														
r	10, 10	−5.0	7.7	−12.6	2.7 / 3.1	31 / 32	0	20, 20	−4.8	22.1	−21.8	2.1 / 2.8	33 / 33	0
	180, 150	−1.9	8.8	−7.7	2.7 / 3.2	32 / 44	0.7	170, 140	−2.5	8.0	−7.5	2.8 / 3.1	29 / 43	8.3
4r	20, 20	−4.6	27.2	−25.0	1.9 / 2.4	38 / 32	0	20, 20	−4.8	28.5	−23.8	1.9 / 2.5	38 / 33	1.8
								60, 40	−4.9	35.7	−26.5	1.7 / 2.2	43 / 26	0
	150, 90	−3.6	10.4	−14.9	2.8 / 2.6	36 / 31	4.7	140, 50	−4.5	19.8	−21.3	2.5 / 2.4	42 / 23	7.7
s16	10, 10	−5.0	12.1	−13.4	2.4 / 2.9	31 / 34	2.0	20, 10	−4.7	22.3	−21.6	2.1 / 2.7	36 / 32	0
	150, 150	−2.1	4.8	−5.3	3.2 / 2.8	41 / 32	3.3							
	180, 150	−1.7	9.8	−5.6	2.6 / 3.3	31 / 45	0	180, 140	−2.1	8.2	−4.1	2.6 / 3.3	28 / 45	8.3
s356	20, 10	−4.8	26.3	−21.4	2.0 / 2.4	39 / 31	0	20, 10	−4.8	27.8	−22.0	1.9 / 2.4	38 / 33	0
	150, 150	−3.0	7.5	−5.8	2.9 / 2.8	38 / 33	7.0	70, 40	−4.9	35.4	−23.2	1.7 / 2.2	42 / 27	0.2
	180, 150	−2.1	9.0	−8.9	2.7 / 3.1	34 / 42	7.1							

Phase angles refer, respectively, to purine (R) and pyrimidine (Y) nucleotides and twists refer, respectively, to RpY and YpR steps. Translations are in Angstromš, rotations in degrees, and energies in kcal / mol.

graphic results commonly contain some B-DNA pyrimidines with O4′-endo puckers, but solution NMR results rarely show high percentages of such conformations (see ref. 22 and references therein).

Although these criteria do not appear to be very strict, many of the calculated maps do not satisfy them. We begin with the Parm91 force field (Table II) and with full phosphate charges (−1, Table II). These results show that the *r* and *s16* dielectrics (Diel.) can be eliminated on the basis of the A minima that show very small Xdisp, strong negative base pair inclination, and very large inter base pair rise. (Canonical values for A-DNA are roughly X-disp = −5 Å, inclination = 20°, rise = 2.6 Å.) The GC map can be seen to be dominated by a hybrid conformation with O4′-*endo* sugars (Fig 2a).

TABLE III.
Stable Helical Conformations with AMBER-94.

	GC							AT						
Diel.	Phase	Xdisp	Inc	Prop	Rise	Twist	ΔE	Phase	Xdisp	Inc	Prop	Rise	Twist	Δ_E
Phosphate Charge −1.0														
r	10, 20	0.9	−14	−4	2.8 / 7.1	26 / 28	8.0	10, 20	1.6	−17	11	2.8 / 7.9	20 / 26	0.3
	150, 150	−2.7	−16	10	4.3 / 3.9	34 / 29	0	140, 140	−3.3	−9	6	3.9 / 3.6	31 / 31	0
4r	20, 20	−4.3	−6	−1.0	3.4 / 4.4	31 / 24	5.9	20, 20	−4.3	−0.3	−7.3	3.0 / 4.0	29 / 28	5.1
	150, 90	−3.5	4	-11.0	3.3 / 3.0	33 / 31	0	150, 140	−2.8	0.4	−11.4	3.2 / 3.0	34 / 34	0
	140, 140	−3.5	−3	−3.4	3.4 / 3.3	36 / 28	0.2	170, 170	−0.5	−14.6	−11.2	3.4 / 3.2	36 / 44	0.8
s16	10, 10	−0.3	−7	−6	2.8 / 6.2	32 / 29	16.7							
	180, 170	−0.7	−5	3	3.6 / 3.4	38 / 41	0	140, 170	−2.2	3	−3	3.1 / 3.6	40 / 29	
s356	10, 10	−3.9	−4.0	−4.0	3.4 / 4.0	32 / 27	7.5	10, 10	−3.9	5	−13	3.0 / 3.6	31 / 32	4.2
	150, 160	−2.5	−2.1	−1.6	3.4 / 3.3	40 / 31	0	150, 150	−3.0	3	−7	3.1 / 3.2	34 / 35	0
	180, 150	−1.7	2.6	−4.0	3.2 / 3.3	32 / 43	0.3							
Phosphate Charge −0.5														
r	10, 10	−3.5	−8.2	−3	3.6 / 4.3	31 / 27	3.3	10, 10	−3.8	−1.0	−8	3.4 / 3.8	30 / 31	2.1
	150, 160	−2.4	−6.0	1	3.6 / 3.4	39 / 31	0	140, 100	−4.2	3.0	−3	3.3 / 3.2	28 / 32	0
	180, 140	−2.0	1.2	−1	3.3 / 3.3	28 / 44	0.3	140, 140	−3.4	2.5	−4	3.2 / 3.2	33 / 32	0.2
4r	20, 20	−4.6	16	−21	2.4 / 3.2	32 / 31	4.1	20, 20	-4.4	19	−23	2.2 / 3.2	33 / 32	5.1
	150, 90	−3.7	10	−14	3.0 / 2.8	35 / 30	0	180, 80	0.2	−14	−47	3.5 / 2.1	29 / 50	0
	150, 140	−3.2	6	−11	3.1 / 2.9	36 / 32	0.8	150, 140	−3.0	4	−13	2.9 / 3.1	35 / 34	3.7
								170, 150	−0.8	−14	−17	3.5 / 2.9	30 / 48	1.3
s16	10, 10	−3.8	1.0	−6.3	3.2 / 4.1	32 / 28	9.3	10, 10	−4.2	13	−15	2.8 / 3.3	32 / 33	0.5
								0,170	−1.5	−1	−1	2.8 / 4.1	24 / 28	0
	150, 170	−2.1	0.9	−0.3	3.4 / 3.2	42 / 29	2.3	130, 160	−2.9	7	−6	2.9 / 3.4	39 / 29	1.0
	190, 150	−1.5	5.0	−2.0	3.0 / 3.4	28 / 46	0	180, 180	1.3	−26	−5	3.3 / 3.2	42 / 48	2.5
s356	10, 10	−4.8	9.2	9.0	2.8 / 3.3	33 / 30	3.7	10, 10	−4.5	20	−17	2 / 3 / 3.0	34 / 34	0
	150, 160	−2.7	3.0	−4.0	3.2 / 3.1	40 / 31	0	140, 150	−3.5	8	−9	2.8 / 3.1	35 / 33	0.7
	180, 150	−1.9	4.8	−5.1	3.0 / 3.2	32 / 43	0.1							
Phosphate charge −0.25														
r	10, 10	−4.8	4.8	−6.0	3.0 / 3.5	31 / 29	2.6	10, 10	−4.6	18.3	−15.2	2.4 / 3.0	33 / 34	0
	150, 90	−4.3	6.8	−2.4	3.2 / 3.0	29 / 32	0							
	150, 160	−2.5	1.0	−1.6	3.3 / 3.2	39 / 31	1.1							
	190, 140	−1.8	5.7	−3.8	3.1 / 3.3	27 / 46	0.5	180, 160	1.0	−25.6	-10.3	3.5 / 3.0	37 / 51	7.3
4r	20, 20	−4.7	30.6	-23.6	2.0 / 2.5	39 / 31	0	20, 10	−4.7	30.7	−23.4	1.9 / 2.5	41 / 29	0.9
	150, 80	−3.8	13.0	−15.3	2.9 / 2.7	36 / 28	2.3	30, 20	−4.6	34.0	−31.6	1.9 / 2.2	42 / 26	0
	90, 150	−3.8	7.0	−8.8	2.8 / 3.2	35 / 27	5.2	140, 130	−3.5	7.3	−14.6	3.0 / 2.9	34 / 32	7.3
								180, 150	0.4	−22.3	−20.0	3.5 / 2.7	32 / 54	7.2
s16	10, 10	−4.9	14.5	−9.4	2.7 / 3.2	32 / 31	3.3	10, 10	−4.7	22.0	−15.8	2.3 / 2.8	34 / 34	0
	190, 140	−1.8	6.6	−2.8	3.0 / 3.3	26 / 46	0							
	140, 170	−2.4	2.5	−1.2	3.3 / 3.1	42 / 27	2.7	190, 170	1.2	−25.7	−5.4	3.3 / 3.2	40 / 51	9.8
s356	10, 10	−5.2	28.0	−12.4	2.0 / 2.4	36 / 34	0	10, 10	−5.2	29.8	−15.2	1.9 / 2.5	35 / 35	0
	150, 160	−2.7	4.2	−4.4	3.1 / 3.0	39 / 31	2.7	140, 140	−3.7	10.6	−9.6	2.8 / 3.0	34 / 33	7.8
	180, 140	−2.2	6.8	−5.8	3.0 / 3.2	30 / 43	1.9	180, 160	0.8	−22.9	−14.6	3.4 / 2.9	37 / 52	10.2

Phase angles refer, respectively,to purine (R) and pyrimidine (Y) nucleotides and twists refer, respectively, to RpY and YpR steps. Translations are in Ångstroms rotations in degrees, and energies in kcal / mol.

For the AT polymer with the *s16* dielectric there is in fact no minimum in the A region. Stronger dielectric damping (*4r* or *s356*) improves the A conformation but does not lead to satisfactory results for B-DNA, all minima having pyrimidines in the O4′-*endo* form (Fig. 2b), coupled with large negative Xdisp and small rise, that is characteristic of a shift toward the A conformation.

The results with reduced phosphate charges (−0.5 table II) also show problems. High dielectric damping (*4r*, *s356*) must be rejected because, with one exception (GC, *s356*), no stable B conformations are found. Low damping is also unsatisfactory because *r* shows no B minimum for AT and *s16* for the same polymer shows a global minimum with hybrid O4′-*endo*/C3′-*endo* sugars. De-

TABLE IV.
Stable Helical Conformations with Flex.

		GC							AT						
Diel.	Phase	Xdisp	Inc	Prop	Rise	Twist	ΔE	Phase	Xdisp	Inc	Prop	Rise	Twist	ΔE
Phosphate charge −1.0														
r	10, 30	0	−29	0	4.0 / 5.3	30 / 30	6.1	10, 20	3.8	−25	19	2.9 / 8.1	17 / 22	0.7
	150, 150	−1.7	−23	19	4.9 / 3.7	36 / 31	0	170, 160	0.5	−15	31	3.4 / 7.1	26 / 33	0
4r	20, 20	−3.4	−10	−5	3.6 / 4.4	29 / 26	2.2	20, 20	−3.7	−10	−5	3.6 / 4.3	28 / 28	2.1
	150, 150	−1.8	−17	8	4.1 / 3.7	36 / 32	0	150, 150	−2.1	−10	0	3.6 / 3.6	34 / 35	0
s16	10, 20	−0.1	−24	−7	3.6 / 5.3	33 / 29	13.4	10, 20	−0.4	−22	−9	4.0 / 4.7	31 / 31	11.1
	160, 170	−1.1	−14	8	3.9 / 3.7	41 / 33	0	180, 160	−1.2	−5	4	3.7 / 3.5	32 / 42	0
s356	10, 20	−2.4	−15	−5	3.7 / 4.7	30 / 28	3.6	10, 10	−3.3	−11	−3	3.8 / 4.1	29 / 29	2.9
	160, 160	−1.2	−17	7	4.0 / 3.7	39 / 34	0	160, 160	−1.6	−8	−3	3.4 / 3.5	36 / 36	0
Phosphate Charge −0.5														
r	10, 20	−1.9	−18	−4	3.8 / 4.9	30 / 28	2.3	10, 20	−2.5	−15	−5	3.9 / 4.4	28 / 30	1.6
	150, 160	−1.4	−19	8	4.1 / 3.8	39 / 31	0	160, 20	−2.2	−4	−4	3.9 / 3.5	39 / 26	0
								150, 150	−2.4	−8	2	3.6 / 3.6	33 / 44	0.8
4r	20, 20	−4.7	8.1	−15.1	2.8 / 3.5	30 / 29	0.5	20, 20	−4.5	13.6	−19.8	2.7 / 3.2	30 / 32	0.3
	160, 20	−2.6	4.0	−10.0	3.7 / 2.8	44.24	0	170, 160	−0.1	−20.0	−7.0	3.6 / 3.4	38 / 45	0
	160, 160	−1.9	−3.0	−5.0	3.4 / 3.2	38 / 35	0.5							
s16	10, 20	−2.1	−13	−7	3.5 / 4.8	30 / 28	4.1	10, 10	−4.2	6.0	−12.0	3.2 / 3.3	30 / 32	3.1
								160, 20	−3.0	5.0	−3.0	3.4 / 3.6	40 / 25	0
	160, 170	−1.1	−13	6	3.8 / 3.6	40 / 33	0	180, 150	−1.6	−2.5	−1.8	3.4 / 3.3	29 / 43	1.6
								150, 160	−2.7	3.0	−4.0	3.1 / 3.3	35 / 33	1.3
s356	20, 20	−4.9	7.8	−12	2.8 / 3.5	30 / 28	0.6	10, 10	−4.5	15	−17.0	2.7 / 3.0	32 / 34	0
	160, 160	−1.8	−9.0	1	3.6 / 3.4	38 / 34	0	150, 160	−2.2	−1	−8.0	3.2 / 3.4	37 / 34	0.5
								180, 160	0.2	−19	−4.9	3.6 / 3.3	36 / 47	0.6
Phosphate charge −0.25														
r	10, 10	−4.2	−1.0	−7.0	3.2 / 3.9	30 / 28	0	10, 10	−4.6	13.2	−14.8	2.8 / 3.0	31 / 33	0
								150, 150	−2.7	−0.3	−5.0	3.2 / 3.3	34 / 34	2.4
	160, 160	−1.3	−15.4	5.6	3.9 / 3.6	38 / 34	0.4	180, 160	0.9	−23.0	−12.9	3.5 / 3.0	37 / 50	4.4
4r	20, 10	−4.8	29.8	−21.8	2.0 / 2.4	39 / 31	0	10, 10	−5.1	29.8	−16.2	2.0 / 2.5	35 / 35	0
								150, 160	−1.9	−3.2	−9.4	3.2 / 3.3	37 / 35	6.0
	160, 160	−2.0	−0.5	−6.6	3.3 / 3.1	38 / 35	5.0	180, 160	0.8	−21.9	−16.7	3.5 / 2.8	37 / 50	4.9
s16	10, 10	−4.5	4.9	−8.8	3.0 / 3.8	31 / 29	0	10, 10	−4.8	19.4	−14.6	2.5 / 2.8	32 / 34	0
								150, 150	−3.2	6.7	−5.0	3.0 / 3.2	34 / 33	5.0
	160, 160	−1.6	−11.6	4.4	3.8 / 3.6	37 / 34	1.2	180, 160	1.0	−23.5	−10.7	3.4 / 3.1	39 / 49	6.8
s356	10, 10	−5.1	28.5	−16.2	2.0 / 2.4	36 / 34	0	10, 10	−5.2	29.5	−13.4	2.0 / 2.4	34 / 36	0
								20, 10	−5.4	31.3	−11.1	1.9 / 2.4	36 / 33	0.8
								150, 160	−2.2	0.0	−8.0	3.2 / 3.3	37 / 34	7.0
	160, 160	−2.0	−4.8	−1.0	3.5 / 3.3	37 / 34	4.9	180, 160	0.4	−20.8	−15.3	3.4 / 2.9	37 / 50	7.4

(Phase angles refer, respectively, to purine (R) and Pyrimidine (Y) nucleotides and twists refer, respectively, to RpY and YpR steps. Translations are in Ångstroms, rotations in degrees, and energies in kcal / mol).

creasing the phosphate charges still further to −0.25 (Table II) does not improve the results. Notably, in the case of the AT polymer, B-form minima only exist for low dielectric conditions and, in this case, are much less stable than the A form.

The results with the Parm94 force field (Table III) confirm that full phosphate charges (−1 Table III) combined with low dielectric damping lead to highly deformed A conformations with large rise and base pair inclination. Indeed, for the AT polymer and *s16* no A form is located at all. Much better results are obtained with high dielectric damping and the A and B forms are satisfactory. A slight preference is given to the *s356* dielectric because it avoids the global minimum containing O4′-*endo* pyrimidine sugars found with *4r* in the case of the GC polymer (Fig. 2c).

Halving the phosphate charge (−0.5, Table III, Fig. 2e) has a minor impact on the high dielectric conformations, beyond a general increase in Xdisp and a decrease in rise. This decrease in rise repre-

sents an improvement for the A conformations, which still had rather large values using full phosphate charges. *4r* is nevertheless unfavorable, leading to global minima containing O4′-*endo* sugars for both polymers. Reducing phosphate charge has a larger effect on low dielectric damping. *s16* now gives acceptable results for both A and B conformations (although the AT polymer has a hybrid C3′-*endo*/C2′-*endo* global minimum). *r* gives good results with the GC polymer, but slightly favors O4′-*endo* sugars within AT. Reducing the phosphate charges further to −0.25 (Table III) leads to more negative Xdisp and decreased rise. A-DNA conformations are stable with all dielectric functions; but although B forms exist for both polymers with all dielectrics except *4r*, they are never the most stable conformations.

Lastly we turn to the Flex force field (Table IV). These results once again confirm that full phosphate charge combined with weak dielectric damping (Table IV) results in strongly deformed A conformations. (Note that for the AT polymer the A form even adopts positive Xdisp, its base pairs being displaced toward the major groove.) With Flex, even high damping (*4r* or *s356*) does not fully solve this problem and although the B conformations are the most stable (Fig 2d), the A conformations of the GC polymer still have unacceptably high rise. The results with halved phosphate charges are generally better (−0.5, Table IV). *4r* and *s356* (Fig 2f) give very similar and acceptable results for both conformations (although *4r* again leads to a hybrid global minimum in the case of the GC polymer). *r* and *s16* are also similar, although *s16* leads to more canonical A conformations by increasing Xdisp and decreasing rise. The GC polymer nevertheless exhibits a high rise and the AT polymer has a hybrid form global minimum, as seen with the Parm94 force field.

Further reducing the phosphate charges (−0.25 Table IV) leads to acceptable A and B conformations for both polymer whatever the dielectric function employed. Indeed, in terms of conformation, the results show very little sensitivity to the degree of dielectric damping. However, for all dielectric conditions, the A-form minima are the most stable.

CONFORMATIONAL SUBSTATES

The above study suggests that Parm94 and Flex force fields can both lead to acceptable results and that preference should be given to halved phosphate charges and preferably to the sigmoidal dielectric function. To make a finer comparison of conformational behavior, we now turn to a less regular sequence with more degrees of freedom. For this purpose we arbitrarily chose a tetranucleotide sequence $(AGAT)_n$ from the data base of all tetranucleotides that we previously constructed.[8,17] This repeating sequence has eight symmetry distinct sugars. Although it now becomes impossible to map the complete energy hypersurface, we can locate its stable conformational substates using the combinatorial search technique previously described.[17] This approach generates and energy minimizes starting structures with all combinations of the S, X, and E sugar puckers that were found to uniquely characterize all the energy minima located by using JUMNA and the Flex force field. This study was carried out with the Flex and Parm94 force fields, halved phosphate charges, and either the *s*16 or *s*356 sigmoidal dielectrics.

The results show several general features. First substates appear to be characterized by their sugar puckering for the Parm94 force field in the same way as with Flex. As shown in Table V, no two substates share the same sugar conformations. This table also indicates that the number of substates diminishes (by 12 for Parm94 and by 9 for Flex) as the dielectric damping is increased (*s16* → *s356*). In the case of Parm94, the combinatorial search also generates a considerable number of substates (5 for *s356* and 15 for *s16*) with unusual $\alpha\gamma$ backbone conformations ($g^-g^+ \rightarrow tt$, or, more rarely, g^+g^- with occasional couple $t \rightarrow g^+$ changes in β). These substates, which are less stable than those with canonical backbone conformations, are not shown in Table V. Such conformations are observed in DNA crystals but do not seem to be common in solution.[27,28]

It is also found that hydrogen bonding and stacking interactions are stronger in Parm94 than in Flex by roughly 5−10 kcal/mol. This distinction is maintained for both dielectric conditions, although decreasing the dielectric damping globally strengthens the base pairing while slightly weakening stacking (see Table VI).

The most interesting observation is that for both dielectric conditions, a number of the substates found with Parm94 correspond very closely to those found with Flex. With *s356*, this is true for the two Amber substates that can be superposed on two of the most stable Flex substates. Comparing the double stranded (AGAT) repeating unit using an angular root mean square (RMS; includ-

TABLE V.
Comparison of Substates of (AGAT)*n* for Parm94 and Flex Force Fields.

Parm94	ΔE	Flex	ΔE
Dielectric *s16*			
EXXSSESX	0.00	XXSSSSXX	0.00
EXXSSESE	0.05	SXSXXSXS	0.13
ESSESESX	0.32	XXSESSXX	0.51
XXSEESSX	0.35	SXSEXSXS	0.58
XXSESSXX	0.36	XSXSSESX	1.16
XSSESESX	0.42	XXSSSESX	1.19
XSXSSESX	0.44	SXSXXSES	1.55
XXSESESX	0.50	XXSSSSEX	1.72
XSSEESSX	0.74	SXSEXSES	1.89
XXSESSEE	1.15	XXSESSEX	2.06
XSSESSSX	1.25	SXSEESES	3.48
XXSEESEE	1.32	SXSXESES	3.69
XSSESSEE	1.53	XSXSSSXX	5.76
SXSXXSXS	1.60	XSSESXXX	6.58
SXXXXESS	1.73	XSXSSSEX	6.83
SXSXXSES	1.93		
XSXSXESN	2.50		
XSXSSSEE	2.51		
Dielectric *s356*			
XXXSSSSX	0.00	XXSSSSXX	0.00
XXXSSESX	0.24	XSXSSESX	0.79
		SXSEXSXS	1.03
		XXSESSXX	1.16
		SXSEESXS	1.57
		SXSEXSES	1.94
		SXSEESES	2.65

Arrows indicate identical substates. Substates are labeled by their sugar puckers in the order AGAT.TCTA. Energies in kcal/mol.

ing α, β, γ, ε, ζ, χ, P, A for each nucleotide) yields values of 6° and 7°, respectively. These values are very small and represent excellent agreement between the two force fields. (For comparison, the RMS fit between two different substates obtained with given force field is typically between 15° and 50°.) With *s16*, five Amber substates are found to superpose on Flex substates, with RMS values ranging from 5° to 8°. These correspondences are indicated by arrows in Table V.

TABLE VI.
Average Base Pairing and Stacking Energies (kcal / mol) Within $(AGAT)_n$ as a Function of Dielectric Damping.

	Parm94		Flex	
Property	*s16*	*s356*	*s16*	*s356*
Pairing AT	18	12	13	9
Pairing GC	37	22	28	15
Stacking	16	17	9	11

TWISTING AND STRETCHING RIGIDITY

As a final step we compare the overall rigidity of DNA with experimental results for the B conformation as a function fo force field and base sequence. The results (Table VII) list the bending rigidity, B (deduced from Young's modulus Y using the isotropic rod formula, $\pi R^4 Y/4$, with a DNA radius R of 10 Å) and the twisting rigidity, C. The Young's modulus was obtained by fitting a quadratic function to a stretching deformation curve for each of our test polymers and the twisting rigidity was obtained in a similar way from a twist deformation curve.

TABLE VII.
Bending (B) and Twisting (C) Rigidities ($\times 10^{-19}$ erg cm) as Function of Force Field and Base Sequence (for Dielectric (*s356*).

	Parm94	Flex
Bending (B)		
GC	3.6	1.3
AT	3.4	2.7
Twisting (C)		
GC	4.6	5.0
AT	4.9	4.5

The results show that these macroscopic indices exhibit little base sequence dependence. The dielelectric conditions also have little impact, because when passing from *s356* to *s16*, the decreased damping only causes a 5–10% increase in the values (note phosphate charges of -0.5 were used for all calculations).

As for the energy mapping and substate searches discussed above, both the Parm94 and Flex force fields lead to rather similar values, although the AMBER results show somewhat more rigidity with respect to stretching. Both sets of values are compatible with available experimental measurements: B $\cong 1\text{–}3 \times 10^{-19}$ erg cm (see refs. 29, 30) and C $\cong 1\text{–}4 \times 10^{-19}$ erg cm (see refs. 31, 32).

Discussion

The general features of the force fields and the solvent/counterion models can be deduced most easily from the energy mapping studies. First it is found that conformational sensitivity to the dielectric function decreases as atomic charge distribution becomes less polar (Parm91 → Parm94 → Flex). This same trend is seen as the net charge on the phosphate is reduced. The phosphate charge also has an important impact on the energy landscape. While full charges of -1.0 favor B-DNA, -0.5 results in a rough equilibrium between the two allomorphs and -0.25 favors the A form. The dielectric function has less effect on this equilibrium, although higher damping generally stabilizes the B form. It was also noted that strong phosphate charges must be opposed by strong dielectric damping in order to obtain acceptable A-DNA conformations. These factors can be easily linked to the narrow major groove in the A form, which results in enhanced intrastrand electrostatic repulsion.

These observations can explain a number of trends seen in earlier energy minimization and molecular dynamics simulations using versions of the Parm91 force field. When explicit counterions (generally sodium with an increased radius to mimic a first hydration shell) were used,[33] DNA was generally seen to move toward the A-like conformations.[34, 35] This appears to correspond to our results with strongly neutralized phosphate groups. In the case of a dynamics simulation starting from the EcoRI complex conformation, the transition to A-DNA could be avoided by constraining the counterions to remain farther from the double helix. This again seems to be in line with the observed stabilization of the B form for less screened phosphates.

In the absence of explicit counterions or reduced phosphate charges, stabilizing B-DNA requires stronger dielectric damping and good results were effectively obtained by energy minimization[36] and molecular dynamics[4, 37] using either *4r* or *s356*. Again in line with the present results, it was noted that these two functions led to similar conformations[4] and tended to favor pyrimidines with O4′-*endo* puckers.[4, 37]

Overall, energy mapping suggests that the new AMBER Parm94 force field performs better with implicit solvent/counterion models than the earlier parameterization, although Parm94 was developed with explicit solvation models in mind. The best results were obtained with the Parm94 and the Flex force fields, using halved phosphate charges and a sigmoidal dielectric function. The similarity of the results obtained with these two force fields, using phosphate charges of -0.5 and either the *s16* or *s356* functions (see, for example, Fig 2e, f) was confirmed by looking at the substates of a relatively complex tetranucleotide repeating polymer; and, under these conditions, both force fields were also shown to yield macroscopic mechanical properties of the DNA duplex in line with experimental data.

Conclusions

Using the possibilities of the internal coordinate modeling program JUMNA, it was possible to make a thorough comparison of the behavior of three force fields capable of treating nucleic acids, Parm91 and Parm94 from the AMBER program and Flex from JUMNA. These tests were carried out for various continuum solvent/counterion

models, enabling the gain connected with a reduced set of variables to be conserved. The comparisons used polymeric DNAs with repeating base sequences and involved adiabatic conformational mapping, substate searches, and the calculation of macroscopic deformability.

The results point to the superiority of the most recent AMBER parameterization, Parm94, and to a surprising degree of similarity with the Flex force field developed for JUMNA, when an optimal choice was made for the parameters of the solvent/counterion model. Given these findings, the extended version of JUMNA should form a useful bridge between internal coordinate and Cartesian coordinate modeling strategies for DNA. Combined with AMBER, this program can now be used to perform rapid conformational searches, provoked large-scale deformations, or create DNA complexes with other molecules, whose dynamic behavior and thermodynamic properties can then be calculated in Cartesian space while maintaining a consistent force field.

Acknowledgments

The authors wish to thank the Association for International Cancer Research (St. Andrews, U.K.) for their contribution to the funding of this project.

References

1. D. M. York, W. Yang, H. Lee, T. Darden, and L. G. Pedersen, *J. Am. Chem. Soc.*, **117**, 5001 (1995).
2. S. Louise−May, P. Auffinger, and E. Westhof, In *Biological Structure and Dynamics* vol. 2, R. H. Sarma and M. H. Sarma, Eds., Adenine Press, New York, 1996, p. 73.
3. M. Prabhakaran and S. C. Harvey, *J. Phys. Chem.* **89**, 5767 (1985).
4. S. Brahms, V. Fritsch, J. G. Brahms, and E. Westhof, *J. Mol. Biol.* **223**, 455 (1992).
5. R. Lavery, in *Structure and Expression Vol.* 3 *DNA Bending and Curvature,* W. K. Olson, R. H. Sarma, M. H. Sarma, and M. Sundaralingam, Eds., Adenine Press, New York, 1988, p. 191.
6. R. Lavery, K. Zakrzewska, and H. Sklenar, *Comput. Phys. Commun.*, **91**, 135 (1995).
7. M. Poncin, B. Hartmann, and R. Lavery, *J. Mol. Biol.*, **226**, 775 (1992).
8. R. Lavery and B. Hartmann, *Biopys. Chem.*, **50**, 33 (1994).
9. B. Hartmann, D. Piazzola, and R. Lavery, *Nucleic Acids Res.*, **21**, 561 (1993).
10. P. Cluzel, A. Lebrun, C. Heller, R. Lavery, J.-L. Viovy, D. Chatenay, and F. Caron, *Science*, **271**, 792 (1996).
11. R. Lavery, H. Sklenar, K. Zakrzewska, and B. Pullman, *J. Biomol. Struct. Dyn.*, **3**, 989 (1986).
12. R. Lavery, I. Parker, and J. Kendrick, *J. Biomol. Struct. Dyn.*, **4**, 443 (1986).
13. S. J. Weiner, P. A. Kollman, D. T. Nguyen, and D. T. Case, *J. Comput. Chem.*, **7**, 230 (1986).
14. W. D. Cornell, P. Cieplak, C. I. Bayly, I. R. Gould, K. M. Merz, Jr., D. M. Ferguson, D. C. Spellmeyer, T. Fox, J. W. Caldwell, and P. A. Kollman, *J. Am. Chem. Soc.*, **117**, 5179 (1995).
15. V. B. Zhurkin, A. A. Gorin, A. A. Charakhchyan, and N. B. Ulyanov, In *Theoretical Biochemistry and Molecular Biophysics*, D. L. Beveridge and R. Leavery, Eds., Adenine Press, New York, 1990, p. 411.
16. S. T. Rao, E. Westhof, and M. Sundaralingham, *Acta Crystallogr. Sect. A*, **37**, 421 (1981).
17. R. Lavery, In *Modeling Biomolecular Structures and Mechanisms*, Proceedings of the 27th Jerusalem Symposium, (Kluwer, Dordrecht, 1995, p. 217.
18. G. S. Manning, *Q. Rev. Biophys.*, **11**, 179(1978).
19. B. E. Hingerty, R. H. Ritchie, T. L. Ferrell, and J. E. Turner, *Biopolymers*, **24**, 427 (1985).
20. V. Fritsch and E. Westhof, *J. Comput. Chem.*, **12**, 147 (1991).
21. V. Fritsch and E. Westhof, *J. Am. Chem. Soc.*, **113**, 8271 (1991).
22. B. Hartmann and R. Lavery, *Q. Rev. Biophys.*, to appear.
23. S. E. Warne and P. L. DeHaseth, *Biochemistry*, **32**, 6134 (1993).
24. V. I. Ivanov, L. E. Minchenkova, B. K. Chernov, P. McPhie, S. Ryu, S. Garges, A. M. Barber, V. B. Zhurkin, and S. Adhya, *J. Mol. Biol.*, **245**, 228 (1995).
25. G. Guzikevich−Guerstein and Z. Shakked, *Nature Struct. Biol.*, **3**, 32 (1996).
26. J. Doucet., J.-P. Benoit, W. B. T. Cruse, T. Prange, and O. Kennard, *Nature*, **337**, 190 (1989).
27. P. Powers, C. R. Jones, and D. G. Gorenstein, *J. Biomol. Struct. Dynam.*, **8**, 253 (1990).
28. C. Karslake, M. V. Botuyan, and D. G. Gorenstein, *Biochemistry*, **31**, 1849 (1992).
29. G. S. Manning, *Biopolymers*, **22** 689 (1983).
30. M. D. Barkley and B. H. Zimm, *J. Chem. Phys.*, **70** 2991 (1979).
31. D. Shore and R. L. Baldwin, *J. Mol. Biol.*, 170, 983 (1983).
32. D. S. Horowitz and J. C. Wang, *J. Mol. Biol.*, 173, 75 (1984).
33. U. C. Singh, S. J. Weiner, and P. A. Kollman, *Proc. Natl. Acad. Sci.* (*USA*), **82**, 755 (1985).
34. J. Srinivasan, J. M. Withka, and D. L. Beveridge, *Biophys, J.*, **58**, 533 (1990).
35. S. Kumar, Y. Duan, P. A. Kollman, and J. M. Rosenberg, *J. Biomol. Struct. Dyn.*, **12**, 487 (1994).
36. M. Orozco, C. A. Laughton, P. Herzyk, and S. Neidle, *J. Biomol. Struct. Dyn.*, **8**, 359, (1990).
37. V. Fritsch, G. Ravishanker, D. L. Beveridge, and E. Westhof, *Biopolymers*, **33**, 1537 (1993).